CrossMark

ORIGINAL RESEARCH PAPER

An uncoupled procedure for performance assessment of slopes in seismic conditions

G. Tropeano[1] · F. Silvestri[2] · E. Ausilio[3]

Abstract To assess the seismic performance of slopes, the simplified displacement-based methods represent a good-working balance between simplicity and reliability. The so-called uncoupled methods permit to account for the effects of deformability and ductility by computing separately the dynamic site response and the sliding block displacements. In this paper the procedure proposed by Bray and Rathje (1998) was revised and adapted to Italian seismicity on a set of subsoil models, representative of the different soil classes specified by the Italian and European Codes. The relationship expressing the decrease of the equivalent acceleration with earthquake/soil frequency ratio was then obtained by means of dynamic 1D seismic response analyses. Statistical correlations between calculated Newmark displacements, significant ground motion parameters and the critical acceleration ratio were also derived. To estimate the reference ground motion parameters necessary for the full implementation of the proposed procedure, literature predictive equations, calibrated on strong motion records of international databases, were revised for the Italian seismicity. These ground motion prediction equations, together with simplified displacements relationships, allowed for developing an original quick procedure to evaluate the seismic slope performance by specifying the probability of exceedance of a threshold displacement, based only on few seismic input motion parameters.

✉ G. Tropeano
  giuseppe.tropeano@unica.it

  F. Silvestri
  francesco.silvestri@unina.it

  E. Ausilio
  ernesto.ausilio@unical.it

[1] Department of Civil Environmental Engineering and Architecture, University of Cagliari, 2 Via Marengo, 09123 Cagliari, Italy

[2] Department of Civil, Architectural and Environmental Engineering, University of Naples Federico II, 21 Via Claudio, 80125 Naples, Italy

[3] Department of Civil Engineering, University of Calabria, 44/B Via P. Bucci, 87036 Rende, Italy

1 Introduction

The current methods to assess the stability or performance of slopes under seismic conditions can be classified in three different categories (Ausilio et al. 2009; Jibson 2011):

1. *pseudo-static:* a conventional limit equilibrium analysis in which the seismic action is represented by an 'equivalent acceleration';
2. *displacement-based analysis:* the permanent displacements induced by earthquake acceleration-time history are calculated by the rigid sliding block model (Newmark 1965);
3. *stress–strain analysis:* it is possible to account for the spatial variability of ground motion, as well as of the heterogeneity and of the stress-strain behaviour of slope materials.

In the first two cases, soil deformability and coupling between dynamic response of the system and the frequency content of the seismic motion are not considered. Such approximation can be misleading, since the dynamic coupling may produce resonance phenomena and asynchronous motion, with consequent increase or reduction of the inertial effects with respect to those calculated under the hypothesis of rigid behaviour of the slope (e.g. Makdisi and Seed 1978). In principle, these effects can be correctly taken into account through dynamic stress-strain analyses including advanced constitutive models. However, such rigorous approaches need the determination of a number of soil parameters that are often difficult to be measured. Therefore, their use is typically convenient only for the analysis of strategic earth structures.

A good-working balance between simplicity and reliability is represented by displacement-based methods accounting for soil deformability in a simple way. These methods can provide equivalent seismic coefficients suitable for a performance-based pseudo-static analysis, and require few synthetic parameters representative of both ground motion and slope geotechnical model (see for instance: Bray 2007; Ausilio et al 2007b; Saygili and Rathje 2008). These approaches are typically addressed to site-specific analyses; moreover, they are rigorously applicable only to 'coherent slides', i.e. the mechanisms pertaining to Category II according to the well-known classification of earthquake-triggered landslides proposed by Keefer (1984).

A dynamic uncoupled analysis should, in principle, consist of two stages:

1. calculation of an equivalent acceleration time history by a seismic response analysis, typically with a linear equivalent soil modelling;
2. evaluation of displacement by integrating the relative motion between the rigid landslide mass and the stable subsoil below the sliding surface.

The statistical processing of the results obtained by the above two-stage simplified analyses, with reference to a specific seismic database, leads to develop straightforward relationships for simplified displacement predictions.

Figure 1 schematically shows the procedure of a simplified uncoupled approach, by generalising the prototype method originally proposed by Bray and Rathje (1998) and considered in this study. The application needs the preliminary definition of the seismic action, in terms of peak reference acceleration, a_g, frequency content (mean period, T_m)
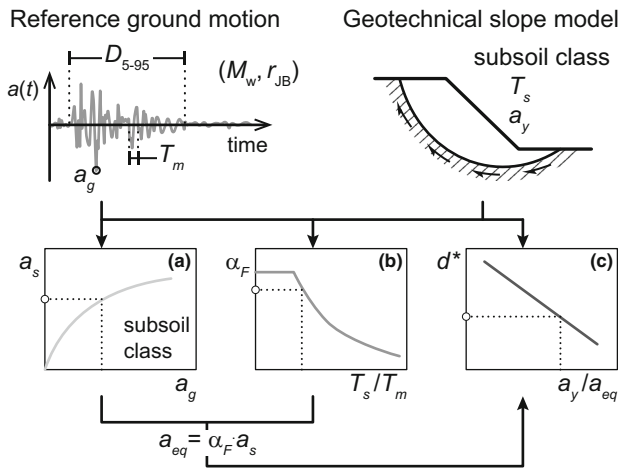
Fig. 1 Flowchart of simplified decoupled approach for evaluating slope permanent displacements

and significant duration of shaking (D_{5-95}, defined between 5–95% normalized Arias intensity). In practice, such parameters can be evaluated by site-specific seismic hazard analyses or empirical predictive relationships (e.g. Rathje et al 2004; Kempton and Stewart 2006). The slope geotechnical model is characterised by the fundamental period, T_s, of the potentially unstable soil mass, and by the yield acceleration, a_y, corresponding to the onset of sliding. Non-linear site amplification is taken into account, by expressing the surface acceleration, a_s, as a function of a_g and of the subsoil class (Fig. 1a); thus, the equivalent acceleration, a_{eq}, is obtained through a reduction factor decreasing with the ratio between T_s and T_m (Fig. 1b). Finally, the value of a_{eq} is used to evaluate the displacement d^*, often normalised with respect to the reference ground motion parameters (Fig. 1c).

In this study, the relationships (a), (b) and (c) in Fig. 1, together with the empirical predictive equations required for estimating the reference ground motion parameters, have been statistically defined for the Italian seismic database (Sect. 2). They have been used to develop a simple screening procedure for the evaluation of seismic performance of slopes from few ground motion parameters defining the design earthquake (Sect. 3). Finally, the different methods described in this paper have been tested for three well-documented case histories (Sect. 4).

2 Simplified decoupled analysis

2.1 Equivalent acceleration

In principle, the time-dependent seismic loading for a slope corresponds to a time history of the equivalent acceleration, $a_{eq}(t)$, proportional to the horizontal resultant of the inertia forces acting on the potentially sliding mass.

In conventional pseudo-static stability analyses, the seismic coefficient is estimated as equal or proportional to the peak value of the equivalent acceleration, $a_{eq,max}$, rather than to the peak ground acceleration of the reference ground motion, a_g, or to that evaluated at surface, a_s. As schematically drawn in Fig. 2a, an operational equivalent acceleration,

$a_{eq}(\approx a_{eq,\max})$, can be defined as the resultant force of the individual peak values of the inertia forces, $F_h(z, t)$, through the expression:

$$a_{eq} = \frac{1}{M} \int_0^H F_h(z)\, dz = \frac{1}{M} \int_0^H \rho\, a_{\max}(z) \cdot b(z)\, dz \tag{1}$$

where M is the soil mass involved in the landslide and ρ is the unit volume mass.

For more complex geometries (i.e. not one-dimensional), a rigorous calculation of a_{eq} requires the use of two-dimensional finite element analyses (e.g. QUAD4M; Hudson et al. 1994). Rathje and Bray (1999) demonstrate that 1-D analyses generally provide a conservative approximation of a_{eq} for deep sliding surfaces and a moderate underestimate for shallow surfaces near slope crests.

When the dynamic equilibrium of a soil column (Fig. 2b) is considered, Eq. (1) can be rewritten as:

$$a_{eq} = \frac{1}{\sigma_v(H)} \int_0^H \gamma\, a_{\max}(z)\, dz \tag{2}$$

that is a conservative evaluation because it does not consider the asynchronous motion.

Therefore, in this study the value of a_{eq} was calculated from the shear stress time history, $\tau(t)$, and the total vertical stress, σ_v, evaluated at the depth, H, of a possible sliding surface:

$$a_{eq} = \max\left[\frac{\tau(H, t)}{\sigma_v(H)}\, g \right] = \frac{\tau_{\max}(H)}{\sigma_v(H)}\, g \tag{3}$$

Following Eq. (3), values of a_{eq} have been obtained from shear stress time history $\tau(t)$, calculated for different possible depths of the sliding surface in a set of virtual soil profiles compatible with the subsoil classification specified by Seismic Eurocode EC8 (EN 1998-1 2003) and the more recent Italian Technical Code (NTC 2008). The computations were carried out through one-dimensional seismic site response (SSR) analyses by using the software EERA (Bardet et al 2000).

2.2 Seismic database

The set of accelerometric records used in this study was extracted from the database SISMA (*Site of Italian Strong Motion Accelerograms*) developed by Scasserra et al. (2008), including 48 Italian earthquakes with moment magnitude, M_w, greater than 4 for the period 1972–2002.
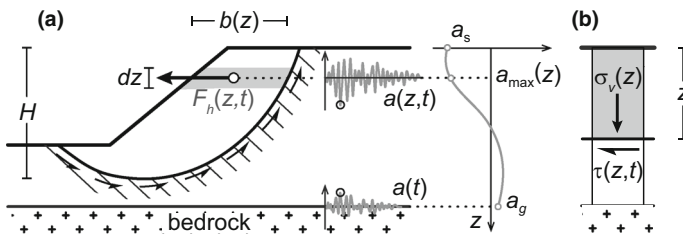

Fig. 2 Calculation of the equivalent acceleration for a circular sliding surface (**a**) and one-dimensional approximation (**b**)

The database consists of 110 recordings from accelerometric stations for which there is availability of a reliable geotechnical characterization. The station sites are classified into three subsoil categories summarizing the site conditions in terms of equivalent shear wave velocity in the shallowest 30 m, $V_{S,30}$. As a result, 40 records were selected for outcropping rock ($V_{S,30} \geq 800$ m/s), 49 records for stiff soil ($360 \geq V_{S,30} > 800$ m/s) and 21 records for soft soil sites ($V_{S,30} < 360$ m/s).

Figure 3a shows the frequency distribution of M_w with reference to the number of records. The magnitude of the selected events has a modal value between 5.5 and 6.5 for the records on rock and soft soil, while for those on stiff soil the modal value is included in the range 4.5–5.5, i.e. that typical of most of the aftershock records of the main Italian seismic sequences.

The horizontal components of the selected records have been processed in order to define the most significant ground motion parameters. The graphs in Fig. 3b, c and d report the frequency distribution of the acceleration peak, a_{max}, the mean period, T_m, and the significant duration, D_{5-95}, for the three subsoil categories described above. The most frequent value of the peak acceleration falls between 0.05 and 0.1 g for all subsoil classes (Fig. 3b), again due to the dominant influence of the aftershock recordings. There is a clear dependence of the mean period on the subsoil class (Fig. 3c): the modal value, in fact, is less than 0.2 s for recordings on outcropping rock and coherently increases for the stiff to soft soil classes; also, the dispersion of the T_m distribution appears to increase with the subsoil deformability. On the contrary, the dependence of the significant duration, D_{5-95}, on soil stiffness is less pronounced (Fig. 3d).
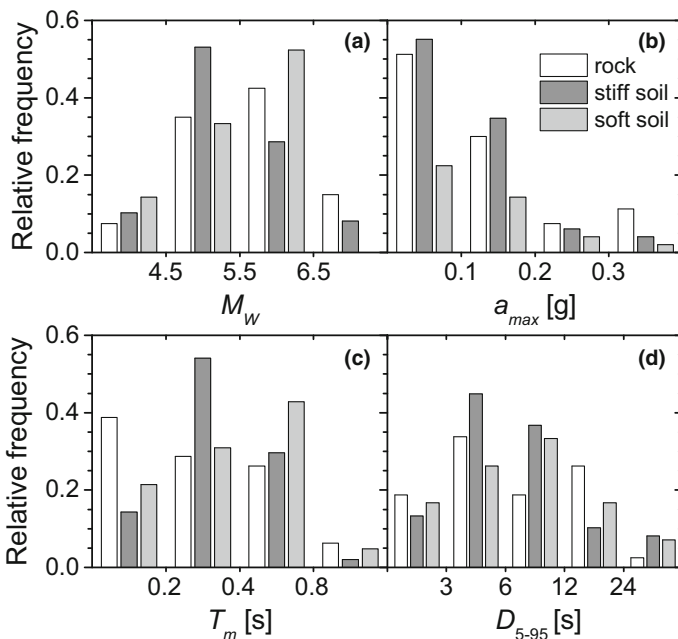
Fig. 3 Frequency distribution of moment magnitude (a), peak ground acceleration (b), mean period (c) and significant duration (d), of the Italian seismic dataset used in this study

2.3 Ground motion prediction equations

The above acceleration-time records were accurately processed obtaining ground motion prediction equations (GMPEs), appropriate to estimate the most significant parameters for calculating the slope displacements, at given earthquake magnitude and source-site distance. In fact, while the peak acceleration, a_g, can be directly specified from the national seismic hazard map, the definition of suitable GMPEs for Italian seismicity is needed for the significant duration, D_{5-95}, and the mean period, T_m.

The simplest forms of the analytical functions proposed by Kempton and Stewart (2006) and Rathje et al. (2004) were considered, excluding the terms accounting for site and directivity effects. Both relationships were derived from the application of the theoretical Fourier spectrum of the source model by Brune (1970, 1971) to a large international strong motion database; in this study, they have been reworked using the 40 records on outcropping rock stations of the Italian database.

In Fig. 4a, b the data points showing the significant duration and the mean period of the Italian accelerograms are compared with the analytical values computed using the GMPEs suggested by Kempton and Stewart (2006) and Rathje et al. (2004), respectively. For D_{5-95}, the GMPE seems to be in agreement with the data, but these latter show a significant scatter, especially for lower magnitude ranges. For T_m, the GMPE tends to overestimate the observations for M_w less than 6.5, and to underestimate them for higher magnitudes.

The GMPE suggested by Kempton and Stewart (2006) can be expressed in a simpler manner introducing constant values of source parameters, obtaining the relationship:
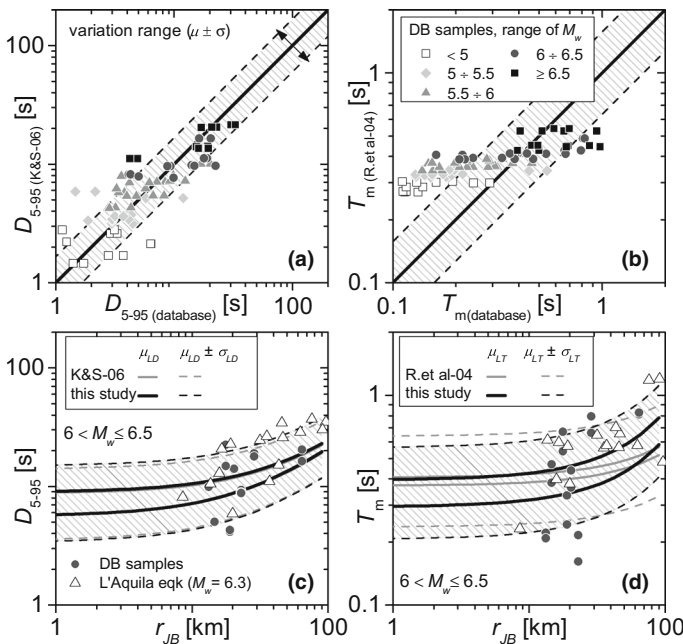
Fig. 4 Comparison between the significant duration (**a**) and the mean period (**b**) of Italian seismic records (DB samples) with those computed through the predictive equations by Kempton and Stewart (2006) (K&S-06) and Rathje et al. (2004) (R.et al-04); comparison of the recorded data with the GMPEs calibrated in this study, for the events with $6 < M_w \leq 6.5$ (**c**, **d**)

$$\log(D_{5-95}) = \log[d_1 \exp(d_2 M_w) + d_3 r_{JB}] + \sigma_{LD} \, \varepsilon_{LD} \tag{4}$$

where r_{JB} is the minimum distance between the site and the fault projection on the ground surface (Joyner and Boore 1981). The suffix LD stands for the random variable obtained as logarithmic transformation of D_{5-95}: therefore, ε_{LD} is the normalized residual error, distributed with a standard normal law, and σ_{LD} is the standard deviation of LD. The regression coefficients d_1, d_2, d_3 and σ_{LD} are reported in Table 1.

In Fig. 4c, the data recorded during events with $M_w = 6 \div 6.5$ (full symbols) are compared with the analytical functions obtained in this study (black lines) and those suggested by Kempton and Stewart (2006), drawn with grey lines.

The median values and the standard deviation predicted by both relationships are practically the same. To verify the reliability of the prediction, the results were also compared to the data from the strong-motion records of l'Aquila earthquake (06/04/2009, $M_w = 6.3$) on rock outcrop, not included in the initial dataset. Although some long distance data fall close to the upper bound, the GMPE by Kempton and Stewart (2006) proves to be enough reliable also for Italian seismicity.

The GMPE suggested by Rathje et al. (2004) was obtained by evaluating the mean period of the Fourier spectrum of the theoretical model, using the source parameters typical of the western US seismicity. Sensitivity analyses by the Authors showed that, for $M_w \leq 7.25$, the dependence of $\log(T_m)$ on both magnitude and distance can be approximated by a linear relationship as follows:

$$\log(T_m) = t_1 + t_2(M_w - 6) + t_3 r_{JB} + \sigma_{LT} \, \varepsilon_{LT} \tag{5}$$

Again, LT is the random variable obtained as logarithmic transformation of T_m, ε_{LT} is the normalized residual error (distributed with a standard normal law), and σ_{LT} is the standard deviation of LT. The coefficients t_1, t_2, t_3 and σ_{LT} are reported in Table 1. As for D_{5-95}, Fig. 4d shows an example of comparison of the data points (full symbols) with the GMPE obtained in this study (black lines) and that originally developed by Rathje et al. (2004), drawn with grey lines, for the magnitude range $6 \div 6.5$. The predictive relationships are, again, compared to the data recorded during l'Aquila earthquake (hollow symbols). Note that the multiple regression of the Italian data significantly improves the parameter prediction. The dependence on M_w was checked as more pronounced, but the residual dispersion was found similar to that reported by Rathje et al (2004). As a

Table 1 Regression coefficients of the GMPEs for significant duration (Eq. 4) and mean period (Eq. 5) proposed in this study

Eq.	Coefficient	Value	Range	SE of coefficient	SD of regression (σ)
(4)	d_1	0.021	± 0.004	0.002	$\sigma_{LD} = 0.221$
	d_2	0.935	± 0.168	0.084	
	d_3	0.156	± 0.057	0.029	
(5)	t_1	-0.532	± 0.069	0.034	$\sigma_{LT} = 0.155$
	t_2	0.256	± 0.061	0.030	
	t_3	0.003	± 0.003	0.001	

Note SE = Standard Error; SD = Standard Deviation

conclusion, Eq. (5) was verified as a satisfactory GMPE for predicting T_m induced by the Italian seismicity.

2.4 Subsoil models

A set of virtual soil profiles, compatible with EC8 and NTC classification criteria, was generated considering different lithologies (Fig. 5a): medium density gravel, sand and soft clay, characterized by thickness varying from 5 to 60 m, and by the index properties listed in Table 2.

The corresponding shear wave velocity profiles were deduced using empirical literature correlations between the small strain stiffness, G_0, and the lithostatic stress state and history (Hardin 1978; Kokusho and Esashi 1981; d'Onofrio and Silvestri 2001); the stiffness parameters were selected as compatible with the soil index properties and the variability range of the empirical relationships.

Thus, a number of 63 soil profiles was obtained; they have been classified into the 4 classes B, C, D, E suggested by EC8 and NTC, according to the combination between the

Table 2 Index properties of the soil types

Soil type	I_P (%)	γ (kN/m³)	e (−)	V_{S30} (m/s)	Class (EC8)
Gravel	0	21	0.3 ÷ 0.7	361 ÷ 797	B
Sand	0	20	0.3 ÷ 1.0	181 ÷ 353	C ($H > 30$ m) − E ($H < 30$ m)
Clay	30	18	–	101 ÷ 174	D ($H > 30$ m) − E ($H < 30$ m)
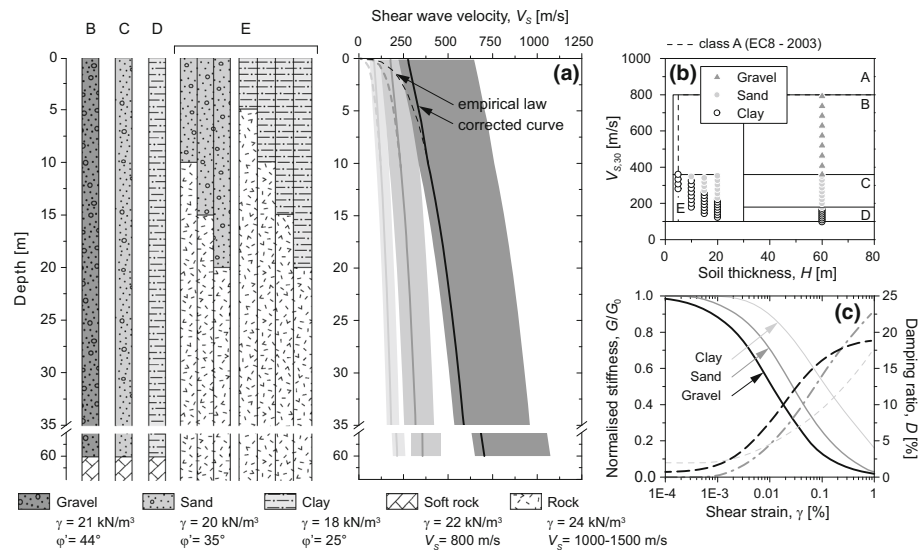
Fig. 5 Virtual subsoil profiles adopted in this study: **a** range of shear wave velocity profiles, **b** EC8 and NTC classification, **c** stiffness and damping curves modified after Vucetic and Dobry (1991) (for sand and clay profiles) and Stokoe et al. (2004) (for gravel profiles)

bedrock depth and the equivalent shear wave velocity (Fig. 5b). The non-linear and dissipative soil behaviour for seismic response analyses was defined expressing the variation of the normalized shear modulus, G/G_0, and the damping ratio, D, with shear strain, γ, through the literature curves reported in Fig. 5c.

The bedrock of the deeper soil profiles, pertaining to class B (gravel), C (sand), and D (clay), was basically assumed as a soft rock with shear wave velocity, $V_{s,b}$, equal to 800 m/s. For the gravel profiles resulting with $V_s > 800$ m/s at the depth of bedrock, the value of $V_{s,b}$ was set equal to that of the overlying soil, in order to avoid inversions and to mitigate the effects of the impedance contrast. These latter are, instead, expected to be more significant for the class E profiles, for which the value of $V_{s,b}$ was imposed equal to 1000 m/s.

2.5 Non-linear response factor

The acceleration records on outcropping rock (described in Sect. 2.2) were assumed as reference input motions for the seismic response analyses. The results were first processed to obtain suitable relationships between the peak acceleration at surface, a_s, and the reference input value, a_g. For each subsoil class, a power law of a_g was considered (Eq. 6):

$$a_s = q \cdot a_g^m \tag{6}$$

Table 3 reports the best fit parameters q and m, together with their statistical variation and the adjusted coefficient of determination, adj.R^2. The non-linear response factor, S_{NL}, can be straightforward defined as follows:

$$S_{NL} = a_s / a_g = q \cdot a_g^{m-1} \tag{7}$$

Figure 6 reports the best-fit curves obtained for each subsoil class together with the sampling distribution regions (symbols and shaded areas). The latter show a dispersion increasing with the shaking intensity, due to the incomplete description of soil response with a unique reference parameter when a marked non-linear soil behaviour occurs. For class E, the large variability of stiffness among the soil columns introduces an additional source of data dispersion.

The same figure shows the comparison between the a_s data (shaded area), the analytical relationships obtained by Eq. (6) (grey lines), and the recommendations by EC8 and NTC (black continuous lines and dashed lines, respectively). Note that, for classes B and E, the relationships obtained in this study are in agreement with the NTC and EC8 indications for input motions of engineering interest ($a_g = 0.1 \div 0.4$ g), while they result less conservative for classes C and, most of all, D.

Table 3 Coefficients of the power law expressing the non-linear response factor, S_{NL} (Eqs. 6–7)

Subsoil class	Equations 6, 7		
	q	m	adj.R^2
B	0.911 ($\pm$0.030)	0.817 ($\pm$0.0197)	0.967
C	0.691 ($\pm$0.035)	0.648 ($\pm$0.0286)	0.890
D	0.598 ($\pm$0.036)	0.654 ($\pm$0.0345)	0.847
E	0.953 ($\pm$0.028)	0.721 ($\pm$0.0170)	0.966
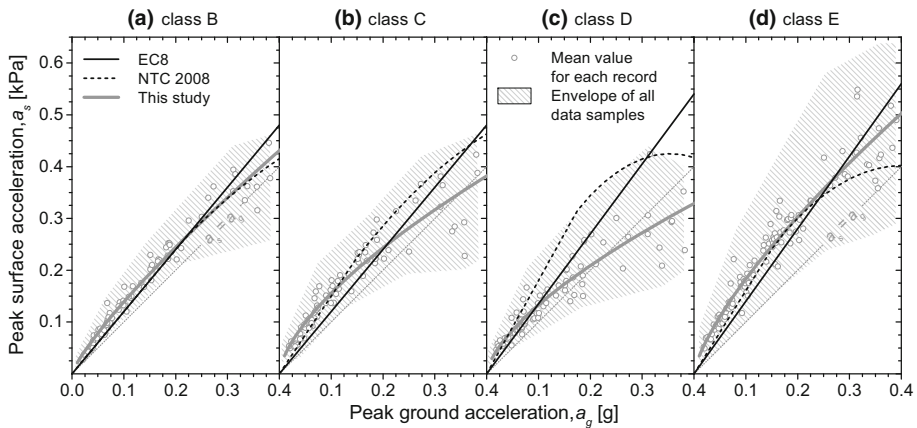
Fig. 6 Regression curves for peak surface acceleration

2.6 Frequency reduction factor

For each dynamic analysis, the equivalent acceleration, a_{eq}, was computed with Eq. (3), referred to a possible sliding surface located at 5, 10, 15, 20, 25 and 30 m, if compatible with the bedrock depth. Following the procedure proposed by Bray and Rathje (1998), for each subsoil class the ratio between a_{eq} and a_s, defined as 'frequency reduction factor', α_F, was expressed as a function of the ratio between the fundamental period of the sliding mass, T_s, and the mean period of the reference ground motion, T_m. This ratio can be easily shown as being proportional to that between the dominant wavelength of the ground motion and the thickness of the potentially sliding mass.

Ausilio et al. (2007a) showed that if the values of a_{eq} and a_s are consistently evaluated, e.g. they both come from the same SSR analysis, the relationship between α_F and T_s/T_m could be considered independent of the subsoil class. The variation of the best-fit curves for each subsoil class, in fact, is lower than the data scatter. Therefore, in this study, the entire available dataset was considered, verifying that the results obtained are in agreement with the observations made by Ausilio et al. (2007a).

A number of 23,360 (63 profiles × 40 input motions × 2 components × 2 to 6 sliding surface depths) values of the frequency reduction factor, α_F, as obtained by as 5040 SSR analyses, was clustered into 13 ranges of T_s/T_m. Statistical analyses were performed to evaluate the distribution of the α_F samples among each subset of data. In particular, the sampling distributions of the logarithm of α_F, for each cluster (shown in Fig. 7 through histograms) could be well described by a normal distribution of the theoretical random variable, LA (grey lines). The logarithmic transformation of α_F for each cluster can be expressed as a function of the normally distributed error, ε_{LA}, as follows:

$$\log \alpha_F = \mu_{LA} + \sigma_{LA}\, \varepsilon_{LA} \tag{8}$$

In Eq. (8), by adopting the well-known 'method of moments', the expected value of LA, μ_{LA}, is set equal to the mean value of the data samples, as well as σ_{LA} is set equal to their standard deviation.

The mean value is expressed as a function of the period ratio by:
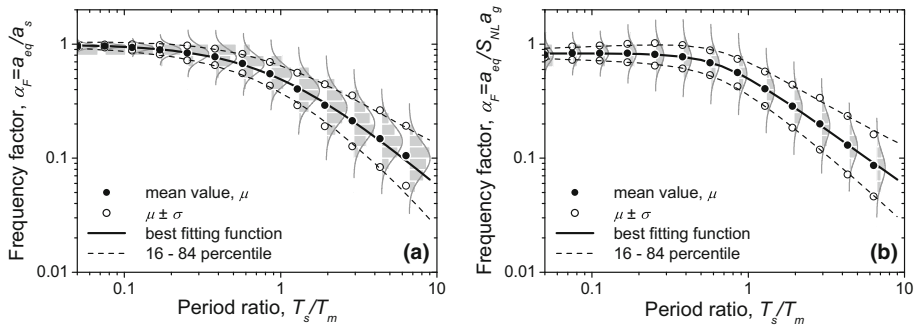
Fig. 7 Frequency reduction factor versus normalized fundamental period of the sliding mass, considering the peak acceleration at surface as computed with SSR analysis (**a**) or using the non-linear response factor (**b**)

Table 4 Regression coefficients for the evaluation of median and standard deviation of the logarithm of the frequency factor (Eqs. 9, 10)

Parameter	Coefficient	(a) a_s from SSR Value (±SE)	(b) a_s from Eq. (6) Value (±SE)
μ_{LA}	a_0	0.000 (±0.000)	−0.081 (±0.003)
	a_1	−0.925 (±0.134)	−0.340 (±0.050)
	θ	0.896 (±0.155)	0.648 (±0.043)
	s	1.260 (±0.064)	2.845 (±0.296)
	adj.R^2	0.999	0.828
σ_{LA}	h	0.118 (±0.006)	0.143 (±0.004)
	k	0.489 (±0.036)	0.375 (±0.020)
	adj.R^2	0.964	0.976

Note SE = Standard Error

$$\mu_{LA} = a_0 + a_1 \log\left[1 + \left(\frac{T_s}{T_m}\frac{1}{\theta}\right)^s\right] \tag{9}$$

in which a_0 is the limit value of $\log(\alpha_F)$ as the period ratio approaches to 0. This latter condition corresponds to a rigid response of the soil column, hence theoretically α_F equal to unity. The parameters θ, a_1 and s are three shape parameters.

The standard deviation increases with the period ratio with a power law:

$$\sigma_{LA} = h \cdot (T_s/T_m)^k \tag{10}$$

Table 4 reports the coefficients of Eqs. (9) and (10), their standard error referred to a 95% confidence level and the adjusted coefficient of determination, adj.R^2.

In Fig. 7a, the sampling data are compared with the regression curve of the mean value (continuous black line) and those referred to 16 and 84% probability of exceedance, i.e. setting $\varepsilon_{LA} = \pm 1$ in Eq. (8) (dashed black lines).

In practice, the maximum surface acceleration, a_s, can be viewed as a random variable, too. For such a reason, an additional set of reduction coefficients was computed using the peak surface acceleration predicted through Eq. (6). The coefficients of the best-fit relationships (9) and (10) were therefore recalculated including the variability of the non-linear

response factor, S_{NL} (see column b in Table 4 and black lines in Fig. 7b). In this case, the data scatter with respect to the mean prediction is increased. Note, also, that a_0 is less than the theoretical zero value: this is due to an overestimation of site amplification for stiff soil columns.

From the above results, an operative relationship simpler than Eq. (8) can be formulated to predict α_F:

$$\alpha_F = \begin{cases} 0.5\,(T_s/T_m)^{-7/8}10^{\sigma_A^*\varepsilon_A} & \text{if} \quad \alpha_F < \alpha_{F,\max} \\ \alpha_{F,\max} = 0.4\,p + 0.65 & \text{if} \quad \alpha_F \geq \alpha_{F,\max} \end{cases} \tag{11}$$

in which p is the probability of non-exceedance and σ_A^* is set equal to 0.25, i.e. about the mean value of the standard deviation in the sampling range of T_s/T_m.
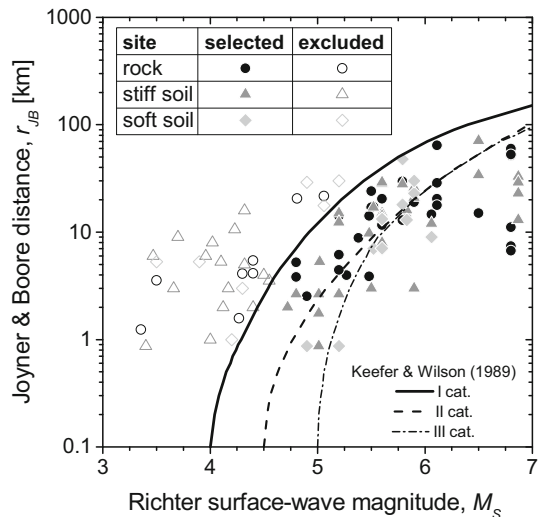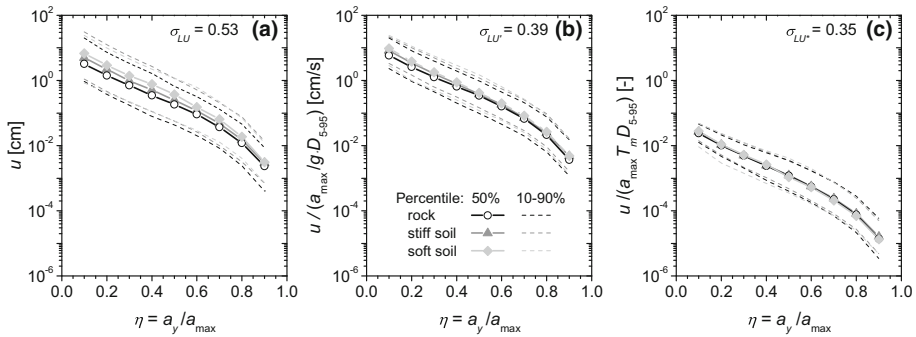
2.7 Displacement relationships

For the prediction of permanent displacements with the rigid block model (Newmark 1965), a screening criterion of the accelerometric data set was introduced, in order to exclude the records not significant for triggering sliding phenomena. The accelerograms excluded from the reference database were those recorded at a source-site distance greater than the limit indicated by Keefer and Wilson (1989) for disrupted slides and falls (i.e. category I in Fig. 8). The final data set consisted of 32 recordings for rock outcrop, 32 for stiff soil, and 14 for deformable soil sites.

Four values of displacements were computed for each one of the above records, since both horizontal motion components (typically, EW and NS), and both up-slope and down-slope directions were considered. The ratio, η, between the yield acceleration, a_y, and the maximum value of the time history along the integration direction, $a_{\max}$, varied from 0.1 to 0.9. For each series of η, the displacement samples, u, were considered as realizations of a random variable, U.

Figure 9a shows the median displacement values (symbols and solid lines), as well as 10 and 90% percentiles (dashed lines), plotted versus η for each subsoil class. The plots

Fig. 8 Screening of acceleration records potentially inducing slope displacements

Fig. 9 Relationships predicting permanent displacement as a function of the acceleration ratio considering: **a** absolute displacements, **b** displacement scaling according to Bray and Rathje (1998), **c** normalized displacements

show a great dispersion of the data (also highlighted by the mean standard deviation of samples, σ_{LU}) and the effects of the soil response.

The scatter decreases if additional ground motion parameters are accounted for. For instance, the plots in Fig. 9b show that an appreciable reduction of the mean standard deviation is obtained after scaling the displacement with respect to the peak acceleration and the duration, as suggested by Bray and Rathje (1998); such a choice, however, does not represent a non-dimensional solution. Therefore, the statistical processing of the data was reviewed looking for a rational normalisation criterion, with the aim to obtain a lower data dispersion. This can be achieved through two ways:

1. a statistical approach, based on the identification of the set of ground motion parameters that minimizes the misfit with the prediction of dynamic Newmark analysis (e.g. Saygili and Rathje 2008);
2. an analytical approach, based on the theoretical solution of the rigid block model subjected to a simple harmonic accelerogram with peak amplitude a_{max}, duration D_{5-95} and period T_m (e.g. Yegian et al 1991).

This latter approach, which was preferred in this study, leads to a dimensionless relationship between the acceleration ratio, η, and the displacement, normalised as follows:

$$u^* = \frac{u}{a_{max}\, T_m\, D_{5-95}} \tag{12}$$

The statistical tests on the mean values of the grouped samples confirmed the logical coherence of the normalisation criterion, since u^* was found as independent of the subsoil class with a significance level of 10% (see Fig. 9c).

The statistical analyses of the set of normalized displacements showed that the random variable U^* is well described by a log-normal distribution. For each value of the acceleration ratio, η, the logarithmic transformation of U^*, indicated as LU^*, was therefore considered. The mean value, μ_{LU^*}, and the standard deviation, σ_{LU^*}, were computed in order to describe a generic realization of LU^* as a function of the standard error, ε_{LU^*}:

$$\log u^* = \mu_{LU^*} + \sigma_{LU^*}\varepsilon_{LU^*} \tag{13}$$

The mean value was expressed as a function of η by using different analytical models. The simplest is represented by the linear function (LIN—Fig. 10a):
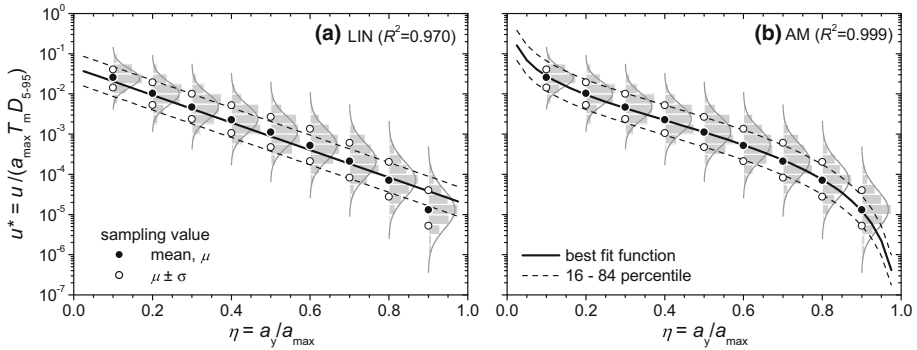
Fig. 10 Statistical distribution of normalized displacement versus acceleration ratio and regression curves considered in this study: **a** linear function and **b** relationship modified from Ambraseys and Menu (1988)

$$\mu_{LU^*} = -1.349 - 3.410\,\eta \tag{14}$$

A second regression law was considered by using the logarithmic relationship proposed by Ambraseys and Menu (1988) (AM—Fig. 10b):

$$\mu_{LU^*} = -2.571 + 2.389\,\log(1 - \eta) - 1.125\,\log(\eta) \tag{15}$$

The corresponding standard deviation, σ_{LU^*}, showed a poor variability with η, which can be expressed through a linear function:

$$\sigma_{LU^*} = 0.25\,(1 + \eta) \tag{16}$$

with an average value approximately equal to 0.35.

In Fig. 10a, b, the distributions of data samples (histograms and grey lines), the median values and the 16th and 84th percentiles (symbols) are compared to the analytical relationships of Eqs. (14) and (15) (black lines), respectively. In particular, the 16th and 84th percentile curves (black dashed lines) were obtained from Eq. (13), by introducing the average value of σ_{LU^*} and setting ε_{LU^*} equal to ± 1. The AM relationship provides the best value of the regression coefficient; however, this curve has two vertical asymptotes for η approaching 0 (i.e. unstable slope in static conditions) and 1 (i.e. acceleration below the critical value).

Therefore, Eq. (15) is ideally applicable for the range $\eta = 0.1 \div 0.9$. On the other hand, Eq. (14) presents a good fit to the sample values for the range $\eta = 0.1 \div 0.5$. The differences between the two laws do not significantly affect the value of the standard deviation evaluated from the residual analysis.

3 Development of a screening procedure

3.1 Displacement hazard curve

The decoupled procedure proposed above, if adopted together with the GMPEs reported in Sect. 2.3, allows to compute a 'displacement hazard curve' for a specific slope.

The displacement hazard curve can be defined as the frequency of occurrence, expressed in terms of a return period or annual rate of exceedance, related to a given displacement. It

includes the probabilistic variation of the parameters characterizing the site seismicity, expressed in terms of relevant 'seismic hazard' curves. The 'design earthquake', instead, can be obtained reversing the hazard analysis by fixing a probability value or a return period. Commonly, for a given site, the seismic hazard and the design earthquake are specified by official documents, namely a 'hazard map' and the technical design code.

For practical purposes, in this study it was considered more appropriate to express the displacement hazard curve as the probability that the design earthquake, with a given return period, produces a displacement greater than a specified value, u. The joint probability can be expressed formally by the relationship:

$$G(u|M, R, \varepsilon) = \iiint dG(D|M,R) \, dG(T|M,R) \, dG(\alpha_F|T) \, G(u|a_g, D, T, \varepsilon, \alpha_F) \, d\alpha_F \, dT \, dD$$

(17)

where $dG(D|M,R)$ and $dG(T|M, R)$ are the Conditional Probability Density Functions (CPDF) of duration, D, and period, T, respectively, for given values of magnitude, M, and distance, R. Instead, $dG(\alpha_F|T)$ is the CPDF of the frequency factor, α_F, for a given T; $G(u|a_g, D, T, \varepsilon, \alpha_F)$ and $G(u|M, R, \varepsilon)$ are the Conditional Cumulated Distribution Functions (CCDF) of the displacement, for a given set of parameters representing ground motion and site seismicity, respectively.

Note that in Eq. (17) the reference acceleration, a_g, is a deterministic value, expressed as a function of (M, R, ε) through an appropriate attenuation law. The yield acceleration and the fundamental period, summarizing the geotechnical properties in the proposed decoupled procedure, are also considered as deterministic variables. As a consequence, the explicit expression of Eq. (17) must be considered as site-dependent, and does not provide general and more widely applicable indications.

In order to simplify the evaluation of the joint probability, the frequency reduction factor, α_F, can be considered as a deterministic parameter; in this case, its value could be computed by introducing the median value of T_m in Eq. (11). Alternatively, to maintain a conservative approach, α_F can be set as $\alpha_{F,max}$ (equal to 0.85 for $p = 50\%$ or to 1 for $p = 84\%$). Under this assumption, the normalized displacement (see Eq. 12) can be expressed in the form:

$$\log(u^*) = \log(u/a_{max}) - \log(D_{5-95}) - \log(T_m)$$

(18)

Introducing in Eq. (18) the relationships (4) and (5), Eq. (13) can be rewritten as a function of the median values of ground motion parameters, as follows:

$$\log\left(\frac{u}{a_{max} \, \bar{T}_m \, \bar{D}_{5-95}}\right) = \mu_{LU^*} + \sigma_{LU^*}\varepsilon_{LU^*} + \sigma_{LD}\varepsilon_{LD} + \sigma_{LT}\varepsilon_{LT}$$

(19)

where

$$\bar{T}_m = 10^{\mu_{LT}} \quad \text{and} \quad \bar{D}_{5-95} = 10^{\mu_{LD}}$$

(20)

in which μ_{LT} and μ_{LD} are the median value of the logarithmic transformation of duration and period from Eqs. (4) and (5), setting null value for ε_{LD} and ε_{LT}.

Assuming that the spurious correlation between the random variables u, D_{5-95} and T_m is expressed through the empirical laws as a function of magnitude and distance, the normalized displacement is a linear combination of the residual random variables ε_{LU^*}, ε_{LD}

and ε_{LT}, that are theoretically independent. The displacement hazard curve, expressed by Eq. (19), may be therefore rewritten as:

$$\log\left(\frac{u}{a_{\max}\bar{T}_m\bar{D}_{5-95}}\right) = \mu_{LU^*} + \sigma_{tot}\varepsilon_{tot} \tag{21}$$

where the total normalised error, ε_{tot}, is distributed again with a standard normal law, while the global standard deviation, σ_{tot}, is given by:

$$\sigma_{tot} = \sqrt{\sigma_{LU^*}^2 + \sigma_{LD}^2 + \sigma_{LT}^2} = 0.45 \tag{22}$$

3.2 Limit acceleration

Following the approach first proposed by Seed (1979), Eq. (13) can be used to evaluate a limit value of the yield acceleration, a_{lim}, fixing a threshold displacement value, u_{lim}, for an assigned probability level (Fig. 11). Referring to the performance-based design approach, u_{lim} may represent the threshold demand parameter that brings the slope to a limit damage state, specified by either the technical code or the engineer.

By reversing the linear formulation for μ_{LU^*} (Eq. 14), a_{lim} can be expressed in closed form as follows:

$$a_{\lim} = \frac{a_{\max}}{3.410}\left[\sigma_{LU^*}\varepsilon_{LU^*} - 1.349 - \log\left(\frac{u_{\lim}}{a_{\max}T_m D_{5-95}}\right)\right] \tag{23}$$

The maximum acceleration, $a_{\max}$, is given by:

$$a_{\max} = \alpha_F\,S\cdot a_g = \alpha_F\,S_{NL}\,S_T\cdot a_g \tag{24}$$

where S is the global value of the site amplification, obtained by multiplying the nonlinear stratigraphic response factor, S_{NL}, with the topographic amplification factor, S_T.

In Eq. (23), the reference ground motion parameters (a_{max}, T_m, D_{5-95}) are still expressed as deterministic variables. To account for their probabilistic nature, Eq. (23) can be generalized by introducing their median values, as predicted by GMPEs, and the global residual random variable, $\sigma_{tot}\,\varepsilon_{tot}$, instead of that of the normalised displacements, $\sigma_{LU^*}\,\varepsilon_{LU^*}$. In this study, the peak ground acceleration was estimated as a function of magnitude and distance through the attenuation law of Ambraseys et al. (1996), i.e. that adopted in the Italian Seismic Hazard map to evaluate the hazard curves of a_g (Barani et al

Fig. 11 Definition of limit acceleration for a given threshold displacement
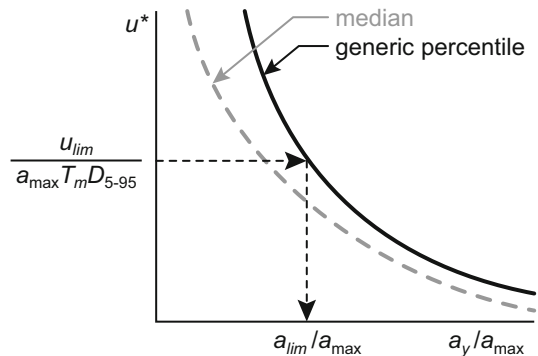
2009). As a result, Eq. (23) can be expressed as a function of magnitude and distance only. The solution cannot be expressed, again, in explicit form, but the limit acceleration can be evaluated as:

$$a_{lim} = \alpha_F S \left\{ a_{lim}^* 10^{0.25\,\varepsilon} + \frac{a_g}{3.41} \left[\log\left(\frac{\alpha_F\, S\, u_{lim}^*}{u_{lim}} \right) + 0.25\,\varepsilon + 0.45\,\varepsilon_{tot} \right] \right\} \qquad (25)$$

In Eq. (25), a_{lim}^* s the 'reference limit acceleration', i.e. the value of a_y which leads a hypothetical reference site not affected by amplification to a threshold displacement, u_{lim}^*, equal to 1 cm, with a probability of 50%. The value of a_{lim}^* can be numerically computed by setting $a_{max} = a_g$ in Eq. (23), for a given magnitude - distance bin. The results are shown in the chart of Fig. 12, where isolines of a_{lim}^* are expressed in terms of Richter surface-waves-magnitude, M_s, and Joyner and Boore distance, r_{JB} (i.e. the parameters requires from GMPE of Ambraseys et al 1996) so as to be compared to the upper bound curves suggested by Keefer and Wilson (1989) for Categories I and II. These latter express the maximum distance at which disrupted or coherent landslides were observed in seismic events, whatever the stability conditions before the earthquake and the amount of permanent displacements of the slopes. Note that the upper bound curve for Category I approximately overlaps the isoline obtained for a_{lim}^* equal to 0.01 g: this latter value can be therefore considered as a lower bound for a_{lim}^*.

Equation (25) accounts also for the error ε needed to correct the median value of ground motion amplitude to the actual value of a_g, obtained by a rigorous evaluation of seismic site hazard; this latter is usually given by the disaggregation data. The same equation also includes the frequency reduction factor, α_F, that can be predicted with Eq. (9), if the fundamental period of the sliding mass is known; if not, a conservative evaluation of α_F can be obtained from Eq. (11), depending on the confidence level adopted.

Fig. 12 Chart for evaluating the reference limit acceleration from hazard evaluated in terms of magnitude and distance. The data points represent the application of the screening criterion for Calitri landslide, Lexington and Austrian dam
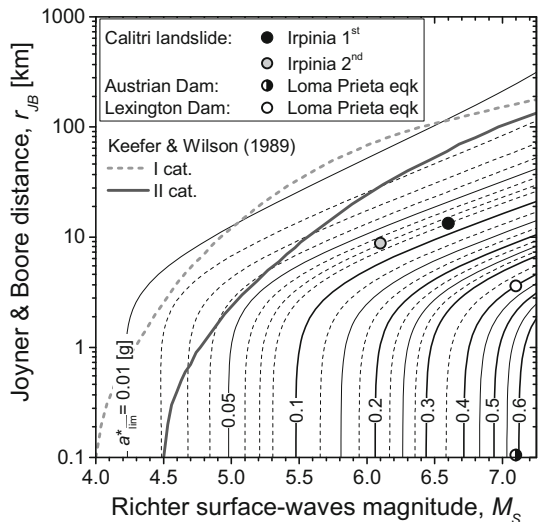
4 Application examples

4.1 The case studies

The two simplified procedures proposed in Sects. 2 and 3 were tested for three well-known case histories, in which permanent displacements were observed during strong-motion earthquakes, and for which the available acceleration records and geotechnical parameters were adequately reliable.

In such conditions, it was possible to perform the simplified analyses with two different approaches with increasing level of detail:

1. a 'seismological approach', i.e. estimating the ground motion parameters by using only source and site information together with ground motion prediction equations;
2. a 'deterministic approach', i.e. using the reference ground motion parameters measured/assumed at the site.

The first case history analysed is a large slope movement in the Calitri village, in Southern Italy (Fig. 13a). The dominating mechanism is a rotational sliding, evolving to a mud-slide at the toe where the slope approaches the left side of Ofanto river valley (Cotecchia and Del Prete 1984; Hutchinson and Del Prete 1985). The slope movement was reactivated by the two sequential main-shocks of Irpinia earthquake, occurred on November 23, 1980 (Irpinia 1st with $M_w = 6.9$, Irpinia 2nd with $M_w = 6.2$), with incremental displacements observed ranging from 1 to 2 m (Hutchinson and Del Prete 1985). At this site, the acceleration time histories were recorded by a station located at the crown of the landslide, where a detailed geotechnical characterisation was available (Palazzo 1993). Due to the location, the records are affected by topographic and stratigraphic amplification; for such a reason, a reference acceleration time history was inferred by an equivalent linear deconvolution analysis through the subsoil profile (Ausilio et al 2009). The ground motion parameters required for the simplified analyses with the second approach were computed from the acceleration time history projected along the azimuth 203.25°, corresponding to the direction of the main movement. The subsoil model of the landslide was calibrated in previous studies including the application of different numerical methods (e.g. Ausilio et al 2009; Tropeano et al 2016). Since the recorded seismic motion and the observed displacements are available for the site, and being the subsoil model adequately characterized, the Calitri landslide was often used for testing predictive relationships and numerical methods proposed by different authors (e.g. Romeo 2000; Lenti and Martino 2013; Tropeano et al. 2016).

The other two examples considered are first-rupture cases damages suffered by two earth dams during the Californian Loma Prieta earthquake on October 18, 1989 ($M_w = 6.9$).

The Austrian Dam (Fig. 13b) is located along the Northern segment of the fault considered responsible for the event, about 11 km away from the epicentre.

After the seismic event, significant sliding phenomena in the proximity of the right abutment were observed: the settlement of the embankment crest was about 75 cm for most part of its length, while the average downstream horizontal displacement was 15 cm, with a maximum value of about 32 cm near the right abutment (Harder et al. 1998). The displacements measured and the damage observed along the embankment foot suggested that a main failure mechanism occurred in the downstream direction.
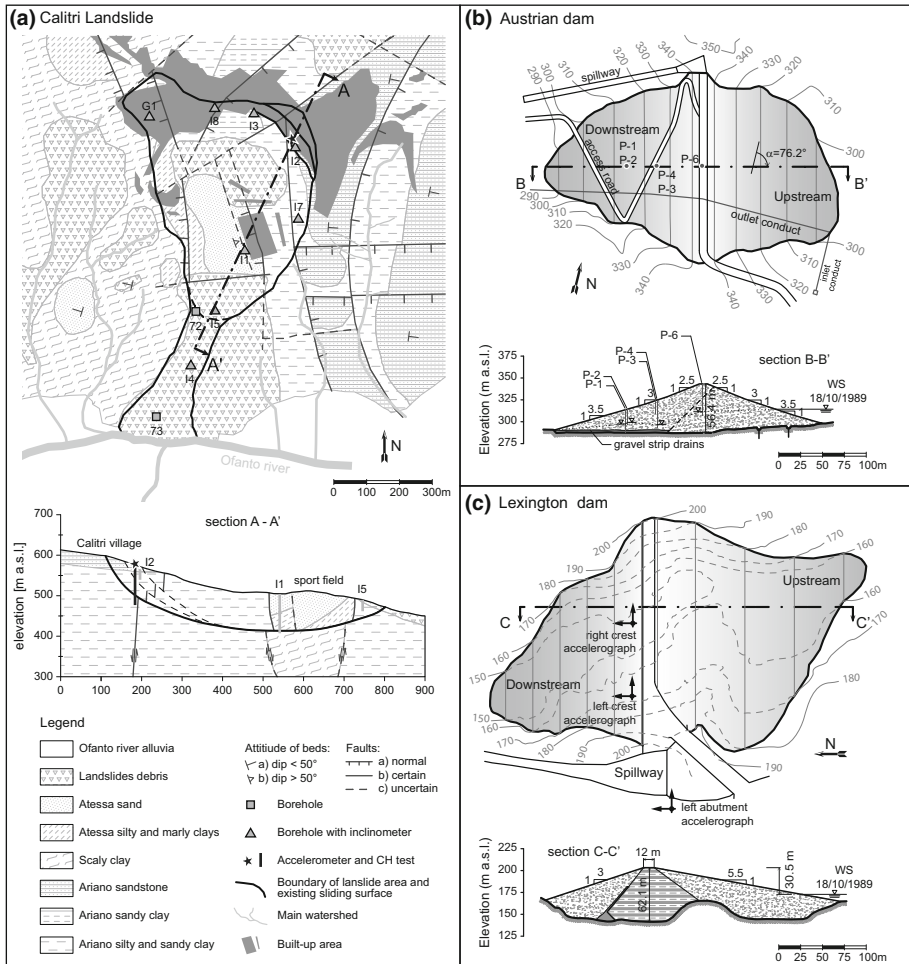
Fig. 13 Plan and main section of **a** Calitri landslide (modified from Martino and Scarascia Mugnozza 2005), **b** Austrian Dam and **c** Lexington Dam (modified from Harder et al. 1998)

The dam was not equipped with any instrument recording the seismic motion, so that, following Vrymoed and Lam (2006), the reference input motion was assumed equal to the record taken at Corralitos station (located about 8 km from the epicenter) projected along the dam cross-section.

The synthetic parameters required for the deterministic approach were computed from the acceleration vector projected along an azimuth equal to 76.2°, corresponding to the downstream direction of the main embankment section. The yield acceleration was computed by pseudo-static analyses, considering the soil parameters and the hydraulic conditions (including the increment in pressure head measured by piezometers after the event), reported by Harder et al. (1998). The predominant period was evaluated following the simplified procedure suggested by Bray (2007).

The Lexington Dam (Fig. 13c), currently known as Lenihan Dam, is a zoned embankment, located at about 3.6 km from the margin of the fault responsible of the Loma Prieta earthquake. The seismic event produced cracks in the upstream and

downstream sides of both abutments. The maximum vertical deformation at the crest was about 26 cm, while the average downstream horizontal displacement was about 4.7 cm and the maximum value was about 7.6 cm near the crest midpoint (Harder et al 1998; Hadidi et al. 2014). The Lexington Dam, at the time of the event, was instrumented with three strong-motion accelerometers, one over the outcropping rock near the left abutment and two on the embankment (left and right crest, see Fig. 13c). These instruments recorded peak accelerations in the direction perpendicular to the axis of the dam (NS) equal to 0.45, 0.39 and 0.45 g, respectively. As highlighted by Harder et al. (1998), the left abutment recording cannot be considered as reference ground motion for the dam, because it presented a significant amplification at low frequencies. This suggests that the recorded motion might be affected by site conditions, or that the instruments were involved in the damage observed on the left abutment; thus, for the deterministic approach, the record taken at Corralitos station was again assumed as reference input motion, considering its NS component acting along the dam cross-section. The geotechnical parameters needed for the application of the proposed procedures were taken by previous studies (Harder et al 1998; Hadidi et al 2014; Tropeano et al 2016).

Table 5 summarizes the main parameters characterizing the three case studies.

Table 5 Geotechnical properties, event information and ground motion parameters for the three cases analysed in this study

Parameter	Calitri landslide		Austrian Dam	Lexington Dam
Subsoil class [EC8-NTC]	B		B	B
T_s (s)	0.45[a]		0.33[b]	0.20[d]
a_y (g)	0.01[a]		0.19[c]	0.31[d]
Event name	Irpinia 1st	Irpinia 2nd	Loma Prieta	Loma Prieta
Event date	23/11/1980	23/11/1980	18/10/1989	18/10/1989
Time (UTC)	18:34:53	18:35:30	00:04:15	00:04:15
M_s	6.6	6.1	7.1	7.1
M_w	6.9	6.2	6.9	6.9
r_{JB} (km)	13.3	8.8	0.1	3.2
a_g (g)	0.07[e]	0.08[e]	0.52[f]	0.63[f]
a_g (GMPE) (g)	0.17	0.17	0.81	0.61
$D_{5–95}$ (s)	24.6	18.0	8.0[f]	7.2[f]
$D_{5–95}$ (GMPE) (s)	15.4	8.2	13.4	13.9
T_m (s)	0.76	0.81	0.61[6]	0.48[f]
T_m (GMPE) (s)	0.55	0.35	0.51	0.52
u[g] (cm)	100–200		15–32	4.7–7.6

[a] After Ausilio et al. (2009)

[b] After Bray (2007)

[c] From limit equilibrium analysis, this study

[d] From limit equilibrium analysis, after Tropeano et al. (2016)

[e] From deconvolution of recorded accelerogram, after Ausilio et al. (2009)

[f] from Corralitos record

[g] Mean–max observed displacements

4.2 Evaluation of the limit acceleration

The application of the screening procedure proposed in Sect. 3 was first addressed to evaluate the limit acceleration of the slopes, given a threshold displacement, u_{lim}. To assess the results of the screening procedure, for each case study u_{lim} was set equal to the observed displacement, and the error, ε, of the predictive equation for the peak ground acceleration was set equal to 0 (i.e. the mean predicted value was considered).

Following the seismological approach, by knowing the magnitude and distance values, the chart of Fig. 12 allowed for evaluating the reference limit acceleration shown in the same figure. The actual limit acceleration was computed from a_{lim}^* through Eq. (25). Table 6 reports the relevant parameters and the values of a_{lim} computed by considering a conservative evaluation of α_F ($p = 84\%$).

Using the deterministic approach, the ground motion parameters were evaluated from the acceleration time history recorded or back-figured at each site. In this case, the value of a_{lim} was computed directly using Eq. (23). The results are again reported in Table 6.

The values obtained for a_{lim} represent the conditions for which the slope displacement may be equal to u_{lim} with a given probability level, i.e. a kind of 'slope fragility'. Such conditions occur when the limit acceleration is greater than the yield acceleration (see Table 5), i.e. the cases shown in Table 6 with bold text. Alternatively, the value of a_{lim} (expressed in g) might be used as horizontal seismic coefficient for a pseudo-static stability analysis. The negative values (<0) imply the possibility that the slope can sustain the limit displacements, but this event has a higher non-exceedance probability.

For the Calitri landslide, this procedure was applied individually to both sub-events, since the observed displacements cannot be attributed to a single shaking, because they result from the whole sequence.

Thus, in this case the results of the screening procedure must be considered as only indicative of the slope fragility; Table 6 shows that the deterministic approach gives more conservative predictions of a_{lim} with respect to the seismological approach, being this latter affected by an underestimation of ground motion parameters, especially of the shaking duration (see Table 5). On the other hand, the limit accelerations predicted by the seismological approach for the two dams appear more conservative, being the most significant ground motion parameters (namely, the duration) estimated by the GMPEs higher than those resulting from the records (see Table 5).

Table 6 Screening procedure applied to the selected case histories

Earthquake		Calitri landslide				Austrian Dam		Lexington Dam	
		Irpinia 1st		Irpinia 2nd		Loma Prieta		Loma Prieta	
Displacement: u_{lim} (cm)		50	100	50	100	15	32	4.7	7.6
Seism. appr.	a_{lim}^* (g)	0.09		0.07		0.56		0.41	
	α_F ($p = 84\%$)	0.99		0.78		0.99		0.99	
	a_{lim} (g) ($p = 50\%$)	**0.019**	<0	< 0	<0	**0.333**	**0.246**	**0.355**	**0.311**
	($p = 84\%$)	**0.053**	**0.030**	0.010	<0	**0.452**	**0.365**	**0.450**	**0.406**
Deter. appr.	α_F ($p = 84\%$)	0.99		0.99		0.99		0.99	
	a_{lim} (g) ($p = 50\%$)	**0.011**	<0	0.010	<0	0.178	0.116	0.298	0.253
	($p = 84\%$)	**0.024**	**0.013**	0.025	0.012	0.261	0.200	0.395	0.350

limit acceleration a_{lim}, greater than yield acceleration a_y

4.3 Evaluation of the displacement hazard curve

The prediction of displacement was also performed by following both approaches above described. The displacements hazard curves were evaluated accounting for the frequency reduction factor, α_F, in three different ways, in order to assess the degree of approximation of the relevant assumptions:

- deterministic median value, by fixing the mean period, T_m (Eq. 11);
- deterministic upper bound, by fixing T_m for $p = 84\%$ (Eq. 11);
- full probabilistic prediction (Eqs. 8, 9, 10).

In the first two cases, the hazard curve was computed by Eq. (21), i.e. considering the linear combination of normal random variables, while in the third case, Eq. (17) was numerically integrated for the (M_w, r_{JB}) bins. In all cases, the linear relationship of Eq. (14) was adopted for the prediction of the median displacement. In Fig. 14, the hazard curves obtained for all cases are shown with box-plots that permit to summarize the main confidence values (median, lower and upper quartiles, 10 and 90% percentiles); the box-plots are compared with the ranges of the observed displacement (mean-max, grey-filled areas).

For the Calitri landslide, the displacement hazard assessment accounts for the time history relevant to both sub-events characterizing the Irpinia earthquake; in fact, an overall probability density function (PDF) of displacement was computed as the convolution integral of the PDFs individually computed for both events.

Analyzing in detail Fig. 14, note that with both approaches the displacements are seldom under-predicted if a conservative value of α_F is adopted, while the full probabilistic prediction yields the lowest median value and the highest data dispersion. This latter largely derives from the non-linear dependence of α_F on the mean period.

As expected, the displacements predicted through the 'deterministic approach' are closer to the observed values, especially if the ground motion parameters result from real recordings on the site, as for Calitri landslide.

Following the 'seismological approach', the results are mainly influenced by the assessment of peak ground acceleration (that is still considered as a deterministic variable), but also by the prediction of the significant duration. It follows that this method tends to over-predict the displacements of the dams for the Loma Prieta earthquake (for which D_{5-95} is overestimated than that of recordings assumed in both cases), while the opposite
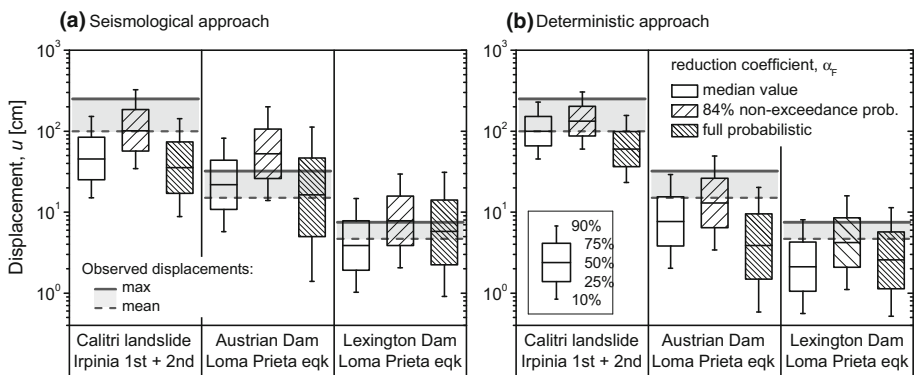
Fig. 14 Comparison between the observed displacements and those predicted following the seismological (a) and the deterministic (b) approaches for the three case histories selected

occurs for the Calitri landslide, being the significant duration of the whole sequence underestimated by the empirical predictive equation.

It must be remarked that the dam displacements are likely to be influenced by other factors that are not considered in the simplified analysis proposed herein, like the cyclic strength degradation and the development of pore water pressure. The latter could be empirically included in the evaluation of yielding acceleration, as it was done in this study for the Austrian dam; this can result in a more conservative estimate of the displacements, but also could increase the uncertainty of the prediction.

5 Discussion and conclusions

The methodology developed in this work allows for implementing the decoupled procedure to calculate seismic slope displacements in fully statistical terms: the required ground motion parameters, in fact, have been defined with appropriate statistical relationships calibrated on the Italian seismicity, such as those directly relating the seismic displacements to the Arias intensity proposed by Romeo (2000). The resulting predictive equations, therefore, allow for evaluating the probabilistic variability of slope displacements, depending on the degree of reliability required for the design.

In order to estimate the reference ground motion parameters required for the full implementation of the proposed procedure, predictive equations for the mean period and the significant duration proposed in literature have been adapted for the Italian seismicity.

The seismic response analyses carried out for evaluating stratigraphic amplification yielded non-linear response factors different than those at present suggested by national and European standards, and, on the average, more sensitive to the reference acceleration (see Fig. 6). The general framework, however, does not lose its validity whether a code-based choice of amplification factor is preferred.

It is widely recognized that the seismic design actions for a slope can be conveniently reduced accounting for the effects of soil deformability, which tends to reduce the resultant of inertia forces due to the asynchronous motion. The possibility of applying a more significant reduction factor to the pseudo-static actions increases with the deformability, and thus the slope vulnerability. However, such possibility is only available if the frequency content of the motion is reliably estimated.

The statistical processing of the dynamic sliding block analyses first of all confirmed the validity of the normalization of permanent displacement with respect to ground motion amplitude, frequency and duration, to reduce the scatter of their dependency on the acceleration ratio.

The knowledge of the statistical distribution of the ground motion parameters has allowed the definition of a 'displacement hazard curve' in terms of joint probability; from this latter, expressions were derived for the prediction of 'limit acceleration' that can be considered as the 'seismic demand' required for the achievement of a given damage level, represented by a threshold displacement. The seismic slope performance can be therefore evaluated by comparing the limit acceleration to the 'seismic capacity', i.e. the yield acceleration. Alternatively, the value of a_{lim} (expressed in g) can be used as horizontal seismic coefficient in the canonical pseudo-static analyses. The procedure requires that the seismic hazard is defined in terms of magnitude distance bins through disaggregation graphs. Provided such data are accessible in the common practice, the simple displacement-based method proposed in this study allows for a more general probabilistic

evaluation of slope stability with respect to the procedures suggested by the Standards, usually expressed in terms of reduction coefficient of the peak acceleration.

The methodologies developed in this work are suitable for site-specific analyses, with some simplified assumptions that can be removed maintaining the practical and straight-forward character of the approach.

The procedures proposed in this study assume a base-sliding mechanism, as well as the original Newmark (1965) approach and related methods for evaluating the permanent displacements. Nevertheless, these methods can be easily extended to different failure mechanisms. Crespellani et al (1998) demonstrated that, for several simple failure mechanisms (infinite slope, wedge, circular and log-spiral sliding surfaces), the permanent displacement can be expressed as the product of the corresponding base-sliding value (namely, that computed considering the yield acceleration of the failure mechanism under investigation) by an appropriate factor dependent on geometrical and mechanical param-eters. These solutions suggest that it is possible to uncouple the probabilistic analysis of a base-sliding mechanism, assumed as a random variable dependent on the seismic motion, from deterministic site-specific factors, depending on slope geometry and soil parameters.

In the dynamic analysis based on the rigid block model, some earthquake-induced phenomena, which can significantly affect the co-seismic displacements (e.g. cyclic degradation of strength parameters and pore water pressure build-up) can be accounted for, in order to improve the reliability of the method. For instance, the accumulation of pore water pressure can be evaluated by relatively simplified models (e.g. Chiaradonna et al. 2016) and this information used for computing a time-dependent yield acceleration, $a_y(t)$. In the simplified predictive relationships, as those calibrated in this study, it is not possible to account for a time variation of a_y, but only for a single representative value, which might be biased by a simplified evaluation of the pore pressure build-up as a function of synthetic ground motion parameters (such as the equivalent number of cycles). However, such dependency should be calibrated on the basis of cyclic laboratory tests, which might be considered as over-sized for such a simplified predictive methods.

In some cases, two- or three-dimensional effects can play a significant role on the focusing of seismic waves and resonance of slopes, as shown by experimental records (e.g. Del Gaudio and Wasosky 2011) and numerical analyses (e.g. Lenti and Martino 2013) on well-documented case studies. In this work, 2D effects were simply introduced in terms of a topographic amplification factor of the maximum acceleration at the surface layer (see Eq. 24), as commonly specified by the technical codes.

For the evaluation of the frequency reduction factor, α_F, Bray (2007) recommendations can be adopted. If the seismic response can be approximated by a one-dimensional motion, Bray (2007) suggests to set T_s equal to $4H/V_s$, where H is the average depth along the slope of the sliding surface, which can be either actual (for a reactivated landslide) or potential (for a first-time failure). In this latter case, the depth of the sliding surface results from the minimization of the yielding acceleration through the conventional pseudo-static methods. Otherwise, T_s might be set equal to the first fundamental period of the 2D elastic vibration mode. The Bray (2007) suggestions are conceptually similar to the heuristic solution proposed by Lenti and Martino (2013).

The procedures can also be used for regional scale applications, in order to provide maps of earthquake-induced displacements, or of the limit acceleration, referring to either deterministic or probabilistic seismic hazard analyses. In such applications, a shakemap, a digital terrain model, geo-referenced soil properties and groundwater depth are required; simplifying assumptions about the failure mechanisms are mandatory, such as the infinite slope model. Typically, the approach followed is limited to the assumption of the rigid

block sliding, neglecting any dynamic coupling (see for instance Silvestri et al. 2016). However, the frequency reduction factor, α_F, can be perspectively included in the computation if T_m can be mapped (e.g. by an appropriate GMPE) and information about the shear wave velocity profile is available (e.g. Forte et al. 2017), at least until the expected depth of sliding surface; if unknown or not even back-figured, this latter can be inferred from the layering and the hydrogeological conditions. As an alternative, α_F can be conservatively set equal to the maximum value 0.85, corresponding to $T_s/T_m < 1$ (see Eq. 11; Fig. 7b).

References

Ambraseys NN, Menu JM (1988) Earthquake-induced ground displacements. Earthq Eng Struct Dynam 16(7):985–1006. doi:10.1002/eqe.4290160704

Ambraseys NN, Simpson KA, Bommer JJ (1996) Prediction of horizontal response spectra in Europe. Earthquake Eng Struct Dynam 25(4):371–400. doi:10.1002/(SICI)1096-9845(199604)25:4<371::AID-EQE550>3.0.CO;2-A

Ausilio E, Silvestri F, Troncone A, Tropeano G (2007a) Seismic displacement analysis of homogeneous slopes: a review of existing simplified methods with reference to Italian seismicity. In: Pitilakis K (ed) IV International conference on earthquake geotechnical engineering, Thessaloniki, Greece, 2007, Thessaloniki, Greece, p paper no. 1614

Ausilio E, Silvestri F, Tropeano G (2007b) Simplified relationships for estimating seismic slope stability. In: Workshop on evaluation committee for the application of EC8, XIV ECSMGE, Madrid, Spain, Madrid, Spain

Ausilio E, Costanzo A, Silvestri F, Tropeano G (2009) Evaluation of seismic displacements of a natural slope by simplified methods and dynamic analyses. In: Kokusho T, Tsukamoto Y, Yoshimine M (eds) 1st International conference on performance-based design in earthquake geotechnical engineering: from case history to practice. CRC Press, Tokyo, pp 955–962

Barani S, Spallarossa D, Bazzurro P (2009) Disaggregation of probabilistic ground–motion hazard in Italy. Bull Seismol Soc Am 99(5):2638–2661. doi:10.1785/0120080348

Bardet JP, Ichii K, Lin CH (2000) EERA a computer program for equivalent–linear Earthquake site response analyses of layered soil deposits. Los Angeles, CA, USA

Bray JD (2007) Simplified seismic slope displacement procedures. In: Pitilakis KD (ed) Earthquake geotechnical engineering, geotechnical, geological and earthquake engineering, vol 6. Springer, Dordrecht, pp 327–353. doi:10.1007/978-1-4020-5893-6_14

Bray JD, Rathje EM (1998) Earthquake-induced displacements of solid–waste landfills. J Geotech Geoenviron Eng 124(3):242–253. doi:10.1061/(ASCE)1090-0241(1998)124:3(242)

Brune JN (1970) Tectonic stress and the spectra of seismic shear waves from earthquakes. J Geophys Res 75(26):4997–5009. doi:10.1029/JB075i026p04997

Brune JN (1971) Correction [to "Tectonic stress and the spectra, of seismic shear waves from earthquakes"]. J Geophys Res 76(20):5002. doi:10.1029/JB076i020p05002

Chiaradonna A, Tropeano G, d'Onofrio A, Silvestri F (2016) A simplified method for pore pressure buildup prediction: from laboratory cyclic tests to the 1D soil response analysis in effective stress conditions. Proc Eng 158:302–307. doi:10.1016/j.proeng.2016.08.446

Cotecchia V, Del Prete M (1984) The reactivation of large flows in the parts of Southern Italy affected by the earthquake of November 1980, with reference to the evolutive mechanism. In: Canadian Geotechnical Society (ed) 4th symposium on landslides, Toronto, Canada, Balkema, Rotterdam, The Netherlands, vol 2, pp 57–62

Crespellani T, Madiai C, Vannucchi G (1998) Earthquake destructiveness potential factor and slope stability. Géotechnique 48(3):411–419

d'Onofrio A, Sivestri F (2001) Influence of micro-structure on small-strain stiffness and damping of fine grained soils and effects on local site response. In: Missouri University of Science and Technology Scholars' Mine (ed) IV international conference on 'recent advances in geotechnical earthquake engineering', San Diego, CA, p paper 15

Del Gaudio V, Wasowski J (2011) Advances and problems in understanding the seismic response of potentially unstable slopes. Eng Geol 122(1):73–83

EN 1998–1 (2003) Eurocode 8: design of structure for earthquake resistance: part 1—general rules, seismic actions and rules for buildings. CEN European Committee for Standardisation, Brussels

Forte G, Fabbrocino S, Fabbrocino G, Lanzano G, Santucci de Magistris F, Silvestri F (2017) A geolithological approach to seismic site classification: an application to the Molise Region (Italy). Bull Earthq Eng 15(1):175–198. doi:10.1007/s10518-016-9960-1

Hadidi R, Moriwaki Y, Barneich J, Kirby R, Moores M (2014) Seismic deformation evaluation of Lenihan Dam under 1989 Loma Prieta earthquake. In: 10th National conference in earthquake engineering, Earthquake Engineering Research Institute, Anchorage, AK

Harder LF, Bray JD, Volpe RL, Rodda KV (1998) Performance of earth dams during the Loma Prieta earthquake. Tech. rep., U.S. Geological Survey, Reston, VA, USA

Hardin BO (1978) The nature of stress–strain behavior for soils. In: Earthquake engineering and soil dynamics-proceedings of the ASCE geotechnical engineering division specialty conference, June 19–21, 1978, Pasadina, CA, ASCE, vol 1, pp 3–90

Hudson M, Idriss IM, Beikae M (1994) QUAD4M-A computer program to evaluate the seismic response of soil structures using finite element procedures and incorporating a compliant base. Davis, CA, USA

Hutchinson J, Del Prete M (1985) Landslides at Calitri, southern Apennines, reactivated by the earthquake of 23rd November 1980. Geologia Applicata e Idrogeologia 20(1):9–38

Jibson RW (2011) Methods for assessing the stability of slopes during earthquakes: a retrospective. Eng Geol 122(1–2):43–50. doi:10.1016/j.enggeo.2010.09.017

Joyner WB, Boore DM (1981) Peak horizontal acceleration and velocity from strong–motion records including records from the 1979 Imperial Valley, California, earthquake. Bull Seismol Soc Am 71(6):2011–2038

Keefer DK (1984) Landslides caused by earthquakes. Geol Soc Am Bull 95:406–421

Keefer DK, Wilson R (1989) Predicting earthquake-induced landslides, with emphasis on arid and semi-arid environments. In: Sadler P, Morton D, Inland Geological Society (eds) Landslides in a semi-arid environment: with emphasis on the inland valleys of southern California. Publications of the Inland Geological Society, Inland Geological Society, Riverside

Kempton JJ, Stewart JP (2006) Prediction equations for significant duration of earthquake ground motions considering site and near-source effects. Earthq Spectra 22(4):985–1013. doi:10.1193/1.2358175

Kokusho T, Esashi Y (1981) Cyclic triaxial test on sands and coarse materials. In: 10th International conference on soil mechanics and foundation engineering, Stockholm, Sweden, vol 1, pp 673–679

Lenti L, Martino S (2013) A parametric numerical study of the interaction between seismic waves and landslides for the evaluation of the susceptibility to seismically induced displacements. Bull Seismol Soc Am 103(1):33–56

Makdisi FI, Seed H (1978) Simplified procedure for estimating dam and embankment earthquake-induced deformations. ASCE J Geotech Eng Div 104(7):849–867

Martino S, Scarascia Mugnozza G (2005) The role of the seismic trigger in the Calitri landslide (Italy): historical reconstruction and dynamic analysis. Soil Dyn Earthq Eng 25(12):933–950

Newmark NM (1965) Effects of earthquakes on dams and embankments. Géotechnique 15(2):139–160. doi:10.1680/geot.1965.15.2.139

NTC (2008) DM 14/1/2008. Norme Tecniche per le Costruzioni. (n.d.). Gazzetta Ufficiale della Repubblica Italiana S.O. n. 30 (n. 20-4/2/2008) (**in Italian**)

Palazzo S (1993) Progetto Irpinia – Elaborazione dei risultati delle indagini geotecniche in sito ed in laboratorio eseguite nelle postazioni accelerometriche di: Bagnoli Irpino, Calitri, Auletta, Bisaccia, Bovino, Brienza, Rionero in Vulture, Sturno, Benevento, Mercato S. Severino (**in Italian**)

Rathje EM, Bray JD (1999) An examination of simplified earthquake–induced displacement procedures for earth structures. Can Geotech J 36(1):72–87. doi:10.1139/t98-076

Rathje EM, Faraj F, Russell S, Bray JD (2004) Empirical relationships for frequency content parameters of earthquake ground motions. Earthq Spectra 20(1):119–144. doi:10.1193/1.1643356

Romeo R (2000) Seismically induced landslide displacements: a predictive model. Eng Geol 58(3):337–351

Saygili G, Rathje EM (2008) Probabilistic seismic hazard analysis for the sliding displacement of slopes: scalar and vector approaches. J Geotech Geoenviron Eng 134(6):804–814. doi:10.1061/(ASCE)1090-0241(2008)134:6(804)

Scasserra G, Lanzo G, Stewart J, D'Elia B (2008) SISMA (site of Italian strong motion accelerograms): a web-database of ground motion recordings for engineering applications. AIP Conf Proc 1020(Part 1):1649–1656. doi:10.1063/1.2963795

Seed HB (1979) Considerations in the earthquake-resistant design of earth and rockfill dams. Géotechnique 29(3):215–263. doi:10.1680/geot.1979.29.3.215

Silvestri F, Forte G, Calvello M (2016) Multi-level approach for zonation of seismic slope stability: experiences and perspectives in Italy. In: Landslides and engineered slopes. Experience, theory and practice, pp 101–118

Stokoe K, Darendeli M, Gilbert R, Menq F, Choi W (2004) Comparison of the linear and nonlinear dynamic properties of gravels, sands, silts and clays. In: Proceedings of the NSF/PEER international workshop on uncertainties in nonlinear soil properties and their impact on modeling dynamic soil response, Pacific Earthquake Engineering Research Center, University of California at Berkeley, Berkeley, CA, USA

Tropeano G, Chiaradonna A, d'Onofrio A, Silvestri F (2016) An innovative computer code for 1D seismic response analysis including shear strength of soils. Géotechnique 66(2):95–105. doi:10.1680/jgeot.SIP.15.P.017

Vrymoed J, Lam W (2006) Earthquake performance of Austrian Dam, California, during the Loma Prieta earthquake, Boston, MA

Vucetic M, Dobry R (1991) Effect of soil plasticity on cyclic response. J Geotech Eng 117(1):89–107. doi:10.1061/(ASCE)0733-9410(1991)117:1(89)

Yegian MK, Marciano EA, Ghahraman VG (1991) Earthquake-induced permanent deformations: probabilistic approach. J Geotech Eng 117(1):35–50. doi:10.1061/(ASCE)0733-9410(1991)117:1(35)